Discriminating between Higgs Boson models using $e^+e^- o t \overline{t} h$ and Zh at the NLC *

J. F. Gunion (U.C. Davis) and X.-G. He (Melbourne)

ABSTRACT

We demonstrate that the process $e^+e^- \rightarrow t\bar{t}h$ at the NLC provides a powerful tool for extracting the $t\bar{t}$ (Yukawa) couplings of the *h*. In combination with the $e^+e^- \rightarrow Zh$ process, an accurate determination of the ZZ coupling of the *h* is also possible. The resulting ability to distinguish different models of the Higgs sector is illustrated by detailed studies for two-Higgs-doublet models.

In extensions of the Standard Model (SM) there are multiple neutral Higgs bosons. Their masses and couplings are often dependent upon many parameters; CP-violating mixing of CP-even with CP-odd neutral Higgs fields is generally possible. Thus, if Higgs boson(s) exist and are discovered at future colliders, it will be extremely important to determine both the magnitude and the CP nature of their couplings[1, 2, 3].

It has been shown that the process $e^+e^- \rightarrow t\bar{t}h$ (h is our notation for a generic neutral Higgs boson) at the proposed Next Linear Collider (NLC) can provide rather accurate determinations of the CP-even and CP-odd tth Yukawa couplings and at least a rough value for the ZZh coupling [3]. The $e^+e^- \rightarrow Zh$ process provides a direct measurement of the ZZh coupling when analyzed in the missing-mass mode with $Z \to e^+ e^-, \mu^+ \mu^-$. Here, we demonstrate that the accuracy with which the couplings can be determined using these two processes will discriminate in a very decisive manner between different models for the Higgs boson sector. By way of illustration, we will consider the general Two-Higgs-Doublet Model (2HDM), for which the masses and couplings of the three neutral Higgs bosons are all free parameters. For simplicity, we focus on the h that is the lightest of the three eigenstates, and assume that it is sufficiently light compared to the other two that $e^+e^- \rightarrow t\bar{t}h$ is not sensitive to the other Higgs states.

The relevant Feynman rules for the Zh and $e^+e^- \rightarrow t\bar{t}h$ processes can be parameterized as:

$$t\overline{t}h: -\overline{t}(a+ib\gamma_5)t\frac{gm_t}{2m_W}, \quad ZZh: c\frac{gm_Z}{\cos(\theta_W)}g_{\mu\nu}, \qquad (1)$$

where g is the usual electroweak coupling constant. For the SM,

$$a = 1, b = 0, c = 1.$$
 (2)

For the 2HDM, the couplings are more complicated. We have

$$a = \frac{R_{2j}}{\sin\beta}, b = R_{3j} \cot\beta, \quad c = R_{1j} \cos\beta + R_{2j} \sin\beta(3)$$

where j = 1, 2, 3 indicates one of the three Higgs mass eigenstates, $\tan \beta$ is the ratio of the vacua of the neutral members of the two Higgs doublets (we assume a type-II 2HDM), and R_{ij} is a 3×3 orthogonal matrix which specifies the transformation between the 2HDM Higgs fields and the Higgs boson mass eigenstates. We employ the parameterization:

$$R = \begin{pmatrix} c_1 & s_1c_3 & s_1s_3 \\ -s_1c_2 & c_1c_2c_3 - s_2s_3 & c_1c_2s_3 + s_2c_3 \\ s_1s_2 & -c_1s_2c_3 - c_2s_3 & -c_1s_2s_3 + c_2c_3 \end{pmatrix} , \quad (4)$$

where $s_i = \sin \alpha_i$ and $c_i = \cos \alpha_i$. Without loss of generality, we identify the lightest Higgs h with the j = 1 mass eigenstate. In this case, we have

$$a = -\frac{s_1 c_2}{\sin \beta}$$
, $b = s_1 s_2 \cot \beta$, $c = c_1 \cos \beta - s_1 c_2 \sin \beta$.
(5)

The *h* has CP-violating couplings if either $ab \neq 0$ or $bc \neq 0$. We make a few remarks based on Eq. (5) regarding special limiting cases.

- In the 2HDM context one can always reproduce the SM couplings of Eq. (2) for any given tan β by taking α₁ = β and α₂ = π. If tan β is not large then determination of tan β would be possible via observation of one of the other Higgs bosons (j = 2, 3). However, if tan β is large then α₁ ~ π/2; coupled with α₂ ~ π, this implies that the remaining Higgs bosons (j = 2, 3) will have small tth couplings, ∝ 1/ tan β, and would not be easily probed via the tth final state.
- At large tan β, b ~ 0 and a ~ c ~ -s₁c₂ (unless s₁c₂ → 0 as in the SM limit); sensitivity to the exact value of tan β is lost and α₁ and α₂ cannot be independently determined.
- For very large tan β ~ m_t/m_b, the bbh couplings can be large, in which case the e⁺e⁻ → bbh rate would be significant and could be analyzed using the procedures to be discussed here for the tth final state.

In this report, we will focus on models with $\tan \beta$ in the vicinity of 1 in order to display the full potential of the $t\bar{t}h$ final state.

The $e^+e^- \rightarrow Zh$ differential cross section is kinematically trivial. The only useful observable is the total cross section, $\sigma_T(Zh)$, which is proportional to c^2 . The differential $e^+e^- \rightarrow t\bar{t}h$ cross section, without measuring the polarizations of the fermions, contains five distinct terms: $\frac{d\sigma}{d\phi} = \sum_{i=1}^{5} c_i f_i(\phi)$, where

$$c_1 = a^2$$
; $c_2 = b^2$; $c_3 = bc$; $c_4 = c^2$; $c_5 = ac$, (6)

^{*}Work supported in part by the Department of Energy, by the Davis Institute for High Energy Physics and by the Australian Research Council.

and the $f_i(\phi)$ are theoretically known functions of the Higgs mass m_h , the machine energy \sqrt{s} , and the final state phase space variables, ϕ , but are not dependent on the model. Note the absence of any term proportional to ab. The $c_3 = bc$ term is explicitly CP-violating. The total cross section, $\sigma_T(t\bar{t}h)$, is a particular linear superposition of the c_i :

$$\sigma_T(t\bar{t}h) = \int \frac{d\sigma}{d\phi} d\phi = c_1 g_1 + c_2 g_2 + c_4 g_4 + c_5 g_5 , \qquad (7)$$

where the g_i are functions of m_h and \sqrt{s} , and specific experimental cuts. There is no contribution from the CP-violating $c_3 = bc$ component of $d\sigma/d\phi$. Since many different Higgs parameter choices can yield any given value of $\sigma_T(t\bar{t}h)$, it is vital to make use of the much greater information embodied in the detailed dependence of $d\sigma/d\phi$ on the ϕ variables.

The statistically optimal technique for extracting the c_i using $d\sigma/d\phi$ was developed in Ref. [3]. One employs weighting functions $w_i(\phi)$ such that $\int w_i(\phi)[d\sigma/d\phi] = c_i$, where the $w_i(\phi)$ are uniquely defined by demanding that the statistical error in the determination of the c_i is minimized; this is the choice such that the entire covariance matrix is at a stationary point with respect to varying the functional forms for the $w_i(\phi)$ while maintaining $\int w_i(\phi)f_j(\phi)d\phi = \delta_{ij}$. The weighting functions are given in Ref. [3]. By employing them, one finds

$$c_i = \sum_k X_{ik} I_k = \sum_k M_{ik}^{-1} I_k , \quad \text{where } I_k \equiv \int f_k(\phi) d\phi ,$$
(8)

with

$$M_{ik} \equiv \int \frac{f_i(\phi) f_k(\phi)}{[d\sigma/d\phi]} d\phi .$$
(9)

If there are experimental cuts that exclude a portion of the phase space in ϕ , they should be included in computing M_{ik} via the $\int d\phi$ appearing in Eq. (9) in order that optimal statistics be achieved in the presence of the cuts. Since the cuts that will be employed are detector dependent and cannot be determined at this time, we have opted to compute M_{ik} in the examples to follow without including any cuts. However, we *will* reduce the total event rate by an overall efficiency factor, the magnitude for which will be chosen so as to reflect a reduction due to cuts.

The covariance matrix corresponding to M_{ik} of Eq. (9) is

$$V_{ij} \equiv \langle \Delta c_i \Delta c_j \rangle = \frac{M_{ij}^{-1} \sigma_T(t\bar{t}h)}{N(t\bar{t}h)}, \qquad (10)$$

where $N(t\bar{t}h) = L_{\text{eff}}(t\bar{t}h)\sigma_T(t\bar{t}h)$ is the total number of events, with $L_{\text{eff}}(t\bar{t}h)$ being the effective luminosity: $L_{\text{eff}}(t\bar{t}h) = \epsilon(t\bar{t}h)L_{\text{total}}$, where L_{total} is the total integrated luminosity and $\epsilon(t\bar{t}h)$ is the efficiency, including branching ratios for the $t\bar{t}h$ to decay into the useful final states. Since identification of the t and \bar{t} requires that one decay semileptonically and the other hadronically, $\epsilon(t\bar{t}h) \leq 2B(t \rightarrow l\nu b)B(t \rightarrow 2jb) \sim 0.44$. Depending upon how the h decays, there may be a further loss for focusing on reconstructable h final state decays. There will also be cuts and detector efficiencies. We adopt the value of $\epsilon(t\bar{t}h) = 0.1$. For the $m_h = 100 \,\text{GeV}$ value that we shall focus on, for which $B(h \rightarrow b\bar{b}) \sim 0.9$ is likely, this is fairly conservative.

In order to compute the expected experimental errors for the c_i , we first compute M_{ik} [using Monte Carlo integration in Eq. (9) without cuts] and thence, via Eq. (10), the covariance matrix V for the given input model. The confidence level with which one can rule out parameter choices different from those of the input model is then determined by the associated χ^2 value:

$$\chi^{2}(t\bar{t}h) = \sum_{i,j=1}^{5} (c_{i} - c_{i}^{0})(c_{j} - c_{j}^{0})V_{ij}^{-1}, \qquad (11)$$

with

$$V_{ij}^{-1} = \frac{M_{ij}N(t\bar{t}h)}{\sigma_T(t\bar{t}h)}.$$
(12)

In Eq. (11), the c_i^0 are the values for the input model and the c_i are functions of the location in a, b, c parameter space of the alternative model, see Eq. (6). Sensitivity of $\chi^2(t\bar{t}h)$ to the a, b, c parameters is thus directly determined by the covariance matrix for a given model. Typically, one finds that sensitivity to $c_1 = a^2$ is largest, while the weakest sensitivity is to $c_3 = bc$.

We note that $\chi^2(t\bar{t}h)$ implicitly includes a contribution due to the difference in $\sigma_T(t\bar{t}h)$ for the input model as compared to the alternative models. In what follows, we shall be implicitly assuming that the only errors in $\sigma_T(t\bar{t}h)$ are the statistical ones as incorporated in $\chi^2(t\bar{t}h)$ in Eq. (11). However, we note that $\sigma_T(t\bar{t}h)$ will be subject to systematic error as well. The main uncertainties arise from the fact that one must observe $t\bar{t}h$ production in one or more particular final states, leading to uncertainty in $\sigma_T(t\bar{t}h)$ to the extent that the t and h branching ratios and/or the detection efficiencies for these particular final state(s) are uncertain. Thus, we will be implicitly assuming that these uncertainties can be kept below the level of the simple statistical uncertainty.

The statistical analysis for the $e^+e^- \rightarrow Zh$ process is completely straightforward. A direct (i.e. independent of Higgs branching ratios) measurement of $c_4 = c^2$ is obtained when the h is isolated via a peak in the $[(p_{e^+} + p_{e^-} - p_Z)^2]^{1/2}$ missing mass distribution, where we require $Z \rightarrow e^+e^-, \mu^+\mu^$ in order to be assured of the cleanest possible analysis and most reliable absolute normalization. The number of Zh events is given by $N(Zh) = L_{\text{eff}}(Zh)\sigma_T(Zh)$, where $L_{\text{eff}}(Zh) = \epsilon(Zh)L_{\text{total}}$, with $\epsilon(Zh)$ being the efficiency for detecting the events using $Z \rightarrow e^+e^-, \mu^+\mu^-$ decays: $\epsilon(Zh) = B(Z \to e^+e^-, \mu^+\mu^-)\hat{\epsilon}(Zh)$. We take $\hat{\epsilon}(Zh) = 0.5$ for the remnant efficiency associated with cuts and overall detector efficiencies. The relative accuracy of the measurement of c_4 is simply given by $1/\sqrt{N(Zh)}$, and thus the χ^2 associated with choosing a value of c_4 that differs from that of the input model value c_4^0 is given by

$$\chi^2(Zh) = \frac{[c_4 - c_4^0]^2}{[c_4^0]^2} N(Zh) \,. \tag{13}$$

The total χ^2 associated with choosing values for *a*, *b* and *c* that differ from the input model values is given by summing the $t\bar{t}h$ and Zh results:

$$\chi^{2} = \chi^{2}(t\bar{t}h) + \chi^{2}(Zh).$$
(14)

We now provide several examples. We take $m_h = 100 \text{ GeV}$ and $\sqrt{s} = 1 \text{ TeV}$. We assume $L_{\text{total}} = 500 \text{ fb}^{-1}$ (as achieved for 2 1/2 years of running at $L_{\text{year}} = 200 \text{ fb}^{-1}$). This gives $L_{\text{eff}}(t\bar{t}h) = 50 \text{ fb}^{-1}$ and $L_{\text{eff}}(Zh) = 16.9 \text{ fb}^{-1}$. Assuming no cuts, the above m_h and \sqrt{s} imply $\sigma_T(Zh) = 13.6c_4^0$ fb, yielding $N(Zh) = 229.3c_4^0$ events for a given input model. For $\sigma_T(t\bar{t}h)$ [see Eq. (7)] we find (fb units)

$$g_1 = 2.70$$
, $g_2 = 0.530$, $g_4 = 0.083$, $g_5 = -0.055$.
(15)

Note the insensitivity of $\sigma_T(t\bar{t}h)$ to ac, and very modest sensitivity to c^2 .

We consider three input model cases:

- SM: We assume that the input model is such that the Higgs has SM couplings, Eq. (2). From Eqs. (2), (7) and (15), we find σ_T(tth) = 2.73 fb, yielding N(tth) ~ 136 for L_{eff}(tth) = 50 fb⁻¹. For L_{eff}(Zh) = 16.9 fb⁻¹ we obtain N(Zh) ~ 229.
- 2HDM(I): We assume that the input model is the 2HDM model with $\tan \beta = 0.5$, $\alpha_1 = \pi/4$, and $\alpha_2 = \pi/4$, yielding a = -1.118, b = 1, c = 0.4088. In this case, as compared to SM couplings, $\sigma_T(Zh)$ is smaller, yielding $N(Zh) \sim 38$, and $\sigma_T(t\bar{t}h)$ is larger, $\sigma_T(t\bar{t}h) = 3.94$ fb, yielding $N(t\bar{t}h) \sim 197$.
- 2HDM(II): We assume that the input model is the 2HDM model with $\tan \beta = 0.5$, $\alpha_1 = \pi/4$, and $\alpha_2 = \pi/2$, yielding a = 0, b = 1.414, c = 0.6325. In this case, as compared to SM couplings, $\sigma_T(Zh)$ is smaller, yielding $N(Zh) \sim 92$, and $\sigma_T(t\bar{t}h)$ is also smaller, $\sigma_T(t\bar{t}h) = 1.09$ fb, yielding $N(t\bar{t}h) \sim 55$.

In all cases, we use Monte Carlo integration to compute M_{ik} as given in Eq. (9), and Eqs. (10) and (12) to compute the matrix V^{-1} ; all depend upon the input c_i^0 . In computing M_{ik} we do not

It is useful to note that the 1σ statistical errors (expressed in percentage terms) in $\sigma_T(t\bar{t}h)$ and $\sigma_T(Zh)$, corresponding to the above-quoted event rates are:

$$SM = 2HDM(I) = 2HDM(II)$$

$$\sigma_T(t\bar{t}h) : \pm 8.6\% = \pm 7.1\% = \pm 13.5\%$$
(16)

$$\sigma_T(Zh) : \pm 6.6\% = \pm 16.2\% = \pm 10.4\%$$

We believe that the systematic errors in $\sigma_T(t\bar{t}h)$ and $\sigma_T(Zh)$ will be smaller than the above numbers given that the detector efficiencies and the relevant t and h branching ratios should be very well known by the time this analysis is performed. This is presumed to be the case in obtaining the numerical results that follow.

The accuracy with which the 2HDM parameters can be determined is illustrated in Figs. 1, 2 and 3. Each figure has

six windows. In each window of the three figures, a filled central region, an empty band, and a filled band may all be visible. The central region is the $\chi^2 \leq 1$ region, the empty band is the $1 < \chi^2 \leq 4$ region, and the outer filled band is the $4 < \chi^2 \leq 9$ region. If no filled central region is visible, the central region being empty, then this means that $\chi^2 \leq 1$ was not possible. If only a completely filled region appears, then $\chi^2 \leq 4$ was not possible. In the three left-hand windows of each of the three figures, results are displayed for the case where the input model is a 2HDM constrained so as to reproduce the SM couplings when $\tan \beta = 0.5$, 1.0 or 1.5. In the right-hand windows we show results for 2HDM(I) with $\tan \beta = 0.5$ and $\tan \beta = 1$ and for 2HDM(II) with $\tan \beta = 0.5$. For all 2HDM(I) [2HDM(II)] parameter choices, $\chi^2 > 9$ if $\tan \beta = 1.5$ [tan $\beta = 1.0$ or 1.5].

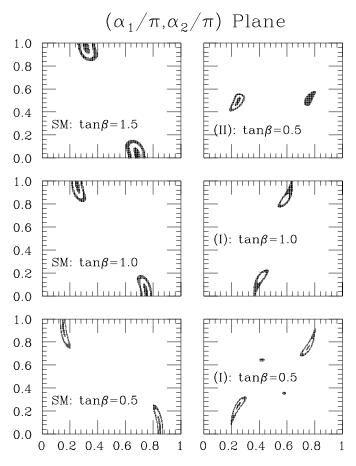


Figure 1: Regions of $\chi^2 \leq 1$, $1 < \chi^2 \leq 4$ and $4 < \chi^2 \leq 9$ in the α_1/π (horizontal axis) and α_2/π (vertical axis) plane. See text for details.

In Fig. 1, we show the above-described χ^2 regions in $(\alpha_1/\pi, \alpha_2/\pi)$ parameter space. We restrict the plot to $0 \le \alpha_1 \le \pi$ and $0 \le \alpha_2 \le \pi$. (Since $d\sigma/d\phi(t\bar{t}h)$ and $\sigma_T(Zh)$ are only sensitive to a^2 , c^2 , b^2 , ac and bc, nothing changes if we simultaneously flip the signs of a, b, c. Restricting to

 $0 \le \alpha_{1,2} \le \pi$ avoids this ambiguity.) Note the fact that for all but 2HDM(II) the regions in the $0 \le \alpha_1 \le \pi/2$ domain are self-similar to the regions in the $\pi/2 \le \alpha_1 \le 1$ domain obtained by $\alpha_1 \to \pi - \alpha_1$ and $\alpha_2 \to \pi - \alpha_2$, which changes the signs of *a* and *c*, but not *b*.

From this figure, we observe the following.

- In the case of SM input couplings, α_{1,2} must lie close to the α₂ = π and α₁ = β values that yield a = c = 1, b = 0, or else to the α₂ = 0, α₁ = π β values that yield a = c = -1, b = 0, leaving a², c², ac unchanged. Note that the different χ² regions all shrink with increasing tan β.
- In the case of 2HDM(I), only tan β = 0.5 (the input value) allows χ² < 1, and the χ² < 1 region corresponds closely to the input α_{1,2} values of α₁ = α₂ = π/4 or the a, c sign-flipped α₁ = α₂ = 3π/4 values. (Self-similarity of the latter χ² regions to the former is a consequence of four facts: i) bc ~ 0.41 is not large; ii) sensitivity of dσ/dφ to c₃ = bc is weak; iii) a² = 1.25 is large; and iv) sensitivity of dσ/dφ to a² is substantial.) If we allow 1 < χ² ≤ 4, the allowed regions expand considerably, and for 4 < χ² ≤ 9 there are two more regions that develop with α_{1,2} values that are very different from the input values. Further, we observe that tan β = 1.0 would be allowed at the χ² > 1 level for yet another region of α_{1,2} values. Values of tan β ≥ 1.5 are excluded at the χ² ≤ 9 level.
- In the case of 2HDM(II), only tan β = 0.5 (the input value) allows χ² ≤ 9. The χ² ≤ 1 region corresponds closely to the input values of α₁ = π/4 and α₂ = π/2. An alternative region with α₁ → π α₁ develops for 4 < χ² ≤ 9. (Self similarity under α_{1,2} → π α_{1,2} is not present since, unlike 2HDM(I), a² = 0 and bc ~ 0.89 is fairly large.)

Note that in the non-SM 2HDM(I) and 2HDM(II) cases we obtain an approximate determination of $\tan \beta$.

The implications for the a, b, c couplings appear in Figs. 2 and 3, in which the χ^2 regions are plotted in the (a, c) and (a, b) planes. All regions with $\chi^2 \leq 9$ are shown in the (a, c)plane figure. In the case of the (a, b) plane, only a > 0 is shown except in the 2HDM(II) case where both the a > 0and a < 0 regions are shown (note the difference in horizontal axis labelling for this case). For the SM and 2HDM(I) cases, a self-similar region to the one displayed for a > 0 is obtained for a < 0 by flipping about the a = 0 axis. (Regions with b < 0 do not emerge.) From the figures, we observe the following.

• For SM input couplings, the output values of a and c must be very close to the a = 1, c = 1 input values, or the alternative a = -1, c = -1 flip, either of which require b > 0. (The $\chi^2 \le 1$ regions are very small dots in the (a, c) plane; careful examination of the picture is required.) The value of b is only moderately wellconstrained when $\tan \beta = 0.5$, with $b \le 0.4$ (0.7) being

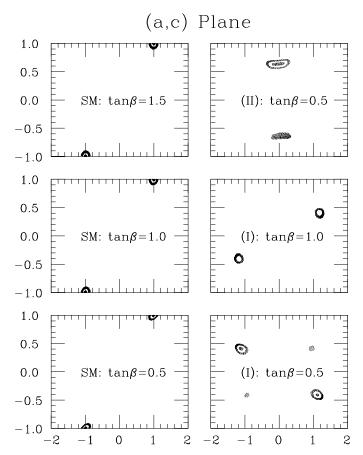


Figure 2: Regions of $\chi^2 \leq 1$, $1 < \chi^2 \leq 4$ and $4 < \chi^2 \leq 9$ in the *a* (horizontal axis) and *c* (vertical axis) plane. See text for details.

allowed at the $\chi^2 \leq 1$ ($\chi^2 \leq 4$) level. The constraint on b becomes much tighter as $\tan \beta$ increases, with $b \leq 0.2$ being required for $\chi^2 \leq 4$ once $\tan \beta \geq 1.5$.

- For 2HDM(I) input, the tan β = 0.5 windows of the (a, c) and (a, b) planes show that the a, b, c couplings are all very well-determined at the χ² < 1 level (up to the sign-flip of a and c). Substantial flexibility in b develops for 1 < χ² ≤ 4. For 4 < χ² ≤ 9, a region where a has changed sign (but not c) develops. For tan β = 1.0, χ² ≤ 1 is not possible, but for 1 < χ² ≤ 4, a solution develops that has the wrong sign of ac and a very distorted value of b. χ² ≤ 9 is not possible for tan β = 1.5.
- For 2HDM(II) input, the a, b, c are again welldetermined if we demand $\chi^2 \leq 1$, and $\chi^2 \leq 4$ allows much less flexibility than in the 2HDM(I) case. However, $4 < \chi^2 \leq 9$ allows a a solution with the flipped sign of ac and slightly distorted b values. [In the (a, b) plane 2HDM(II) window, the three different χ^2 regions associated with the correct sign of ac are some-

what obscured by the strange extra blob associated with $4 < \chi^2 \le 9$ and the wrong sign of ac.]

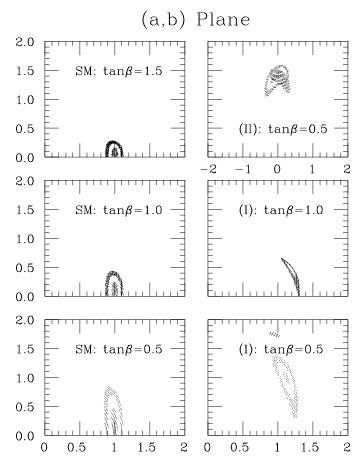


Figure 3: Regions of $\chi^2 \le 1$, $1 < \chi^2 \le 4$ and $4 < \chi^2 \le 9$ in the *a* (horizontal axis) and *b* (vertical axis) plane. See text for details.

In conclusion, we note that it is very possible (some would say probable) that the SM is not correct. In this case, and if there is a weakly-coupled Higgs sector, there will certainly be Higgs bosons that do not have SM-like couplings. This is true even if one neutral Higgs is very SM-like (as for example is very probable in the minimal supersymmetric model), since the others must have very small ZZ coupling and can have all manner of $t\bar{t}$ couplings. Thus, it will be crucial to determine if an observed Higgs boson fits into a given model context, such as the two-Higgs-doublet model, and to determine the model parameters and associated couplings for acceptable solutions. By doing this for all the Higgs bosons we would be able to completely fix the Higgs sector model and parameters.

In this report, we have examined the possibility of carrying out such a program by applying the optimal analysis procedure of Ref. [3] to the $e^+e^- \rightarrow t\bar{t}h$ differential cross

section and measuring the $e^+e^- \rightarrow Zh$ total cross section. Using $L_{\text{total}} = 500 \text{ fb}^{-1}$ of data from the NLC operating with $\sqrt{s} = 1 \text{ TeV}$, we have demonstrated that for models with a reasonable $t\bar{t}h$ event rate the couplings of a 100 GeV 2HDM Higgs boson can be determined with substantial accuracy at the 1σ level. However, for this luminosity some ambiguities begin to arise in the $1 - 2\sigma$ range. Ambiguities at the $< 1\sigma$ level could arise if systematic uncertainties in the experimental determination of the overall normalization of the $t\bar{t}h$ and Zh total cross sections are not small compared to the statistical accuracies. At larger Higgs masses, statistics will deteriorate; higher L_{total} will be required to avoid significant ambiguity. However, even when ambiguities emerge, we have found that they are usually sufficiently limited that the type of analysis presented here will make a critical contribution to gaining a clear understanding of the exact nature of all the Higgs bosons. Certainly, these procedures will provide a powerful means for distinguishing between substantially different models. We urge our experimental colleagues to carry out fully realistic simulations of this type of analysis.

Acknowledgement: Collaboration with B. Grzadkowski in the development of the optimal technique and earlier investigations of the $t\bar{t}h$ process (as summarized in Ref. [3]) is gratefully acknowledged.

REFERENCES

- [1] J.F. Gunion, H.E. Haber, G.L. Kane and S. Dawson, *The Higgs Hunters Guide*, Addison-Wesley Publishing; J.F. Gunion, A. Stange, and S. Willenbrock, *Weakly-Coupled Higgs Bosons*, preprint UCD-95-28 (1995), to be published in *Electroweak Physics and Beyond the Standard Model*, World Scientific Publishing Co., eds. T. Barklow, S. Dawson, H. Haber, and J. Siegrist.
- [2] B. Grzadkowski and J.F. Gunion, Phys. Lett. 294, 361(1992); *ibid*, B350, 218(1995); J.F. Gunion and J.G. Kelly, *ibid*, B333, 110(1994); D. Atwood and A. Soni, Phys. Rev. D45, 2405(1992); *ibid*, D52, 6271(1995); J.F. Gunion and X.-G. He, Phys. Rev. Lett. 76, 4468(1996); S. Bar-Shalom, D. Atwood, G. Eilam, R. Mendel and A. Soni, Phys. Rev. D53, 1162(1996).
- [3] J. F. Gunion, B. Grzadkowski and X.-G. He, Preprint, UCD-96-14, hep-ph/9605326.